Combined electronic structure/molecular dynamics approach for ultrafast infrared spectroscopy of dilute HOD in liquid H_2O and D_2O

Cite as: J. Chem. Phys. **120**, 8107 (2004); https://doi.org/10.1063/1.1683072
Submitted: 26 November 2003 . Accepted: 22 January 2004 . Published Online: 13 April 2004

S. A. Corcelli, C. P. Lawrence, and J. L. Skinner

Combined electronic structure/molecular dynamics approach for ultrafast infrared spectroscopy of dilute HOD in liquid H_2O and D_2O

S. A. Corcelli, C. P. Lawrence, and J. L. Skinner[a)]
Theoretical Chemistry Institute and Department of Chemistry, University of Wisconsin, Madison, Wisconsin 53706

(Received 26 November 2003; accepted 22 January 2004)

We present a new approach that combines electronic structure methods and molecular dynamics simulations to investigate the infrared spectroscopy of condensed phase systems. This approach is applied to the OH stretch band of dilute HOD in liquid D_2O and the OD stretch band of dilute HOD in liquid H_2O for two commonly employed models of water, TIP4P and SPC/E. *Ab initio* OH and OD anharmonic transition frequencies are calculated for 100 $HOD\cdot(D_2O)_n$ and $HOD\cdot(H_2O)_n$ ($n=4-9$) clusters randomly selected from liquid water simulations. A linear empirical relationship between the *ab initio* frequencies and the component of the electric field from the solvent along the bond of interest is developed. This relationship is used in a molecular dynamics simulation to compute frequency fluctuation time-correlation functions and infrared absorption line shapes. The normalized frequency fluctuation time-correlation functions are in good agreement with the results of previous theoretical approaches. Their long-time decay times are 0.5 ps for the TIP4P model and 0.9 ps for the SPC/E model, both of which appear to be somewhat too fast compared to recent experiments. The calculated line shapes are in good agreement with experiment, and improve upon the results of previous theoretical approaches. The methods presented are simple, and transferable to more complicated systems. [DOI: 10.1063/1.1683072]

I. INTRODUCTION

Ultrafast vibrational spectroscopy is emerging as a powerful new tool to complement existing nuclear magnetic resonance-based techniques for probing the structure and dynamics of condensed phase systems of chemical and biological importance.[1–17] Vibrational frequencies are very sensitive to local chemical or solvation environments. For example, observing how the vibrational frequencies of an isotopically labeled residue in a protein evolve as the protein folds or unfolds can provide detailed information regarding the dynamics of the folding process.[18–24] Ultrafast vibrational spectroscopy experiments have been extensively applied to liquid water,[25–42] because of its prominent role as a solvent in a wide variety of interesting chemical and biochemical reactions. These experiments, along with detailed theoretical analysis, have succeeded in connecting the dynamics of spectral diffusion within the OH (or OD) stretching band to hydrogen bond making and breaking dynamics.[43–46] The focus of this article is to present new computational methods to aid in molecular interpretation of these ultrafast infrared (IR) experiments. Although these new methods are applied herein to liquid water, their distinct advantage over existing methods is the ease with which they can be applied to other systems as well.

Most experiments performed to study the vibrational dynamics of water have focused on the OH stretch of a dilute mixture of HOD in liquid D_2O.[29–40] More recent experiments have involved the OD stretch of HOD in H_2O.[25,26,28,47] There are some important experimental and pedagogical reasons to study these systems as opposed to neat liquid water. First of all, in each of these systems the vibrations of interest are spectrally separated from the other vibrational modes. Thus, for example, studying these isotopic mixtures eliminates rapid resonant intermolecular vibrational energy transfer. Second, whereas the symmetric and antisymmetric stretching vibrations of H_2O (D_2O) involve both H (D) atoms, the mass asymmetry in the HOD molecule makes it an excellent approximation to view the OH and OD stretches as being very nearly uncoupled local modes of vibration. Asymmetric solvation environments make this an even better approximation. This significantly simplifies molecular-level interpretation of experiment, since in this case the relevant vibrational frequency perturbations come from one hydrogen bond donor rather than two.

The challenge is to develop a simple theoretical framework in which to understand and analyze these novel experiments, and to connect the measured time scales to details of the molecular structures and motion present in the liquid. Central to any viable method for understanding ultrafast vibrational spectroscopy is the ability to compute the time evolution of the vibrational frequency of interest. A number of different approaches have been devised to calculate the vibrational frequency of a solute molecule in water.[43–46,48–60] These approaches can be divided into two general classes: mixed quantum-classical approaches that use (nuclear) quantum mechanics to determine the vibrational frequencies of the solute molecule in the presence of a solvent that evolves classically,[43–46,48–53] and approaches that empirically relate the vibrational frequencies of the solute to instantaneous solvent configurations.[54–60]

a)Electronic mail: skinner@chem.wisc.edu

The mixed quantum-classical approaches all begin by partitioning the total Hamiltonian, H, into three pieces: one for the solute vibrational degrees of freedom (the system, described by H_s), the translational and rotational degrees of freedom of the solute molecule and the solvent degrees of freedom (the bath, described by H_b), and terms in the Hamiltonian that involve both system and bath variables (the system-bath coupling, described by V). The bath variables are propagated classically using molecular dynamics (MD) simulation with all of the atoms in the solute molecule constrained at their average ground vibrational state positions. At each time step in the MD simulation vibrational frequencies of the solute molecule are determined either by taking diagonal matrix elements of H_s+V (between eigenstates of H_s),[43,44,48,49,53,61] or adiabatically by varying the solute vibrational coordinates over a suitable range (for fixed bath) and solving the resulting Schrödinger equation exactly.[45,46,51,52] Two of us[43,44,48,49,62–65] have improved upon the standard mixed quantum-classical approach by self-consistently renormalizing the system and bath Hamiltonians for a given vibrational state of the solute molecule. In this approach the bath average of the perturbation V is zero. If the main contribution to the solute frequency fluctuations comes from electrostatics, one can approximate the vibrational frequencies for each bath configuration using linear and quadratic Stark shifts.[33,66,67]

The other type of approach involves an empirical relationship between the frequency of the solute and the geometric configuration of the solvent. Buck, Buch, and co-workers[58–60] related the shift in vibrational frequency of a water molecule to the projection of the electric field in the direction of its OH bonds. Their empirical function relating the frequency and electric field was obtained by fitting the experimental infrared spectra of $(H_2O)_7$ and $(H_2O)_8$ clusters. This function was then used to calculate infrared spectra of both smaller and larger water clusters. Cho and co-workers[54–57] have computed the infrared spectrum of the model peptide compound *N*-methylacetamide (NMA) in water by relating the frequency of the amide I mode of the molecule to the electrostatic potential from the solvent at six sites in the molecule (the methyl carbons and each atom of the CONH group). They obtained their relationship by performing a multivariable linear fit to the *ab initio* frequencies of 100 optimized (or nearly optimized) $\mathrm{NMA}\cdot(H_2O)_n$ $(n=1-3)$ clusters.

The approach we take herein is similar in some regards to these last approaches described above, in that, like Buck, Buch, and co-workers[58–60] we parameterize the solvation environment by its electric field, and like Cho and co-workers[54–57] we deterine the vibrational frequencies from *ab initio* calculations involving solute-solvent clusters. One of the main differences, however, is that the clusters we use to obtain the empirical relationship between frequency and electric field are representative of the liquid state. Specifically, the clusters, each containing 5–10 water molecules, are randomly selected from an MD simulation of liquid water and are thus representative of the kinds of solvation environments the HOD molecule experiences in solution. We then use electronic structure methods to compute the OH (OD) stretch vibrational frequency of a HOD molecule solvated in a large number of different D_2O (H_2O) clusters. The vibrational frequencies are calculated by directly generating a one-dimensional potential energy curve for the stretch of interest and then solving the relevant Schrödinger equation. This allows us to calculate the fully anharmonic fundamental vibrational transition frequency without first optimizing the geometry of the cluster. From our cluster results we find that there is (approximately) a linear relationship between the OH (OD) vibrational frequency and the component of the electric field from the solvent molecules in the direction of the OH (OD) bond. This empirical relationship is then used in a standard classical MD simulation to compute important quantities, such as frequency distributions, frequency fluctuation time-correlation functions (TCFs), and vibrational absorption line shapes, the latter two of which have a direct connection with experiment.

The organization of this article is as follows. The components of the computational strategy are described in Sec. II. First, in Sec. II A we discuss how electronic structure methods are applied to small HOD/D_2O and HOD/H_2O clusters to obtain the OH or OD vibrational frequency of the HOD molecule. Then, in Sec. II B we describe how these frequencies are related to the component of the electric field along the OH or OD bond. Third, in Sec. II C we describe details of our MD simulations. The results of the MD simulations of dilute HOD in H_2O and D_2O are discussed in Sec. III. The relationship between the OH or OD stretch vibrational frequency and the length of the hydrogen bond in which the H or D atom participates is discussed in Sec. III A. In Sec. III B the OH and OD frequency fluctuation dynamics are discussed for both the TIP4P and SPC/E water models. OH and OD stretch infrared absorption line shapes for the SPC/E and TIP4P water models are presented in Sec. III C. Finally, concluding remarks are made in Sec. IV.

II. COMPUTATIONAL METHODS

A. Electronic structure

The OH and OD vibrational frequencies of a HOD molecule in small HOD/D_2O and HOD/H_2O clusters were obtained using electronic structure methods. Two sets of clusters were chosen from short MD trajectories of the TIP4P (Ref. 68) and SPC/E (Ref. 69) water models. All of the electronic structure calculations were performed within the GAUSSIAN 98 software package[70] using density functional theory (DFT) with the *B3LYP* functional[71–73] and the $6\text{-}311++G^{**}$ basis set. Since the water clusters come from a room temperature simulation of liquid water, their geometries are far from any local minima, and obtaining the OH or OD vibrational frequency is not simply a matter of performing a harmonic frequency calculation. Instead, we map the *ab initio* one-dimensional potential energy curve for the OH or OD stretch[45,46] and obtain transition frequencies by fitting the curve to a Morse oscillator form whose eigenstates are known analytically.[74] Frequencies obtained in this manner fully reflect the effects of anharmonicity. We suspect this is important because the solvation environment of a HOD

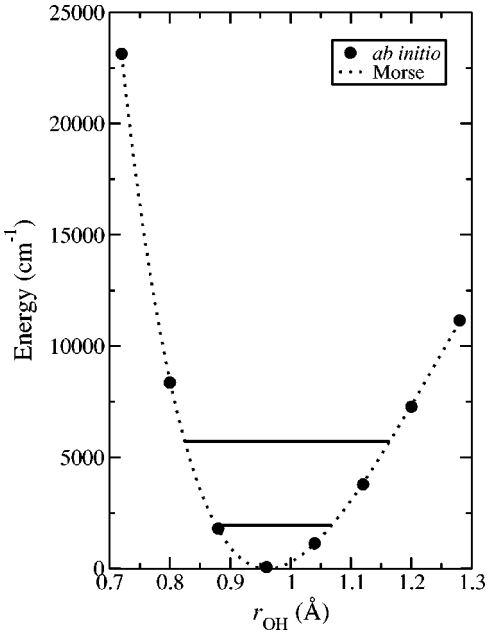

FIG. 1. Potential energy curve for the OH stretch of a HOD molecule in the gas phase. Symbols indicate the results of *ab initio* calculation using the *B3LYP* density functional with a 6-311++G^{**} basis. The dashed line is a fit to the *ab initio* data with a Morse potential energy function [Eq. (1)]. The ground and first excited vibrational energy levels are shown by solid lines.

molecule in liquid water may strongly influence the degree of anharmonicity in the OH and OD stretches.

A simple example of how this procedure was used to obtain the OH vibrational frequency of a single TIP4P HOD molecule in the gas phase is shown in Fig. 1. The closed circles represent the *ab initio* energy of the water molecule as the OH bond is stretched (keeping the angle and the OD bond length fixed at 104.52° and 0.9572 Å, respectively) from 0.72 to 1.28 Å in increments of 0.08 Å. These points were then fit to the Morse potential energy function,

$$V(r)=D(1-e^{-\alpha(r-r_0)})^2, \tag{1}$$

where D is the bond dissociation energy, r_0 is the equilibrium bond length, and α is a parameter that sets the range of the potential. The dotted line in Fig. 1 demonstrates that the calculated potential energy for stretching the OH bond of a water molecule is represented well by the Morse function. A distinct advantage of fitting the potential energy curve to a Morse oscillator is that its vibrational energy levels, E_n, are known analytically and are given by

$$E_n=DB(n+\tfrac{1}{2})[2-B(n+\tfrac{1}{2})], \tag{2}$$

where $n=0,1,2,...$, is the vibrational quantum number, and B^2 is the collection of parameters,

$$B^2=\frac{\alpha^2\hbar^2}{2\mu D}, \tag{3}$$

where μ is the reduced mass of the oscillator. We have assumed that the vibrations of the HOD molecule are comprised of three uncoupled local modes: OH stretch, OD stretch, and HOD bend. For the HOD molecule in the gas phase this is an excellent approximation: an electronic structure calculation of the normal mode eigenvectors of the isolated HOD molecule shows, for example, that more than 98% of the amplitude in OH or OD stretches is attributed to H or D motion, respectively. The local mode approximation becomes even more robust for a HOD molecule in aqueous solution because asymmetric solvation environments further localize the vibrational modes. The reduced masses of the OH and OD stretches of the HOD molecule are simply determined by picturing the molecule as two independent diatomics: H–OD and HO–D. This gives reduced masses of 18/19 amu for the OH stretch and 34/19 amu for the OD stretch. In Fig. 1 the ground and first excited vibrational energy levels are shown for the OH stretch of HOD. Vibrational transition frequencies of the OH and OD stretches in HOD were calculated in this manner to be 3761 and 2775 cm^{-1}, respectively, which compare reasonably well with the experimentally measured values of 3707 and 2724 cm^{-1}.[75] The ratio between the measured and calculated OH and OD vibrational frequencies yields multiplicative scale factors of 0.986 and 0.982, respectively, which can be used to correct systematic errors such as the finite basis set, incomplete incorporation of electron correlation inherent in *ab initio* vibrational frequencies,[76] and errors due to the Morse fitting procedure. All of the OH and OD stretch vibrational frequencies of TIP4P HOD in D_2O and H_2O clusters were corrected using these scale factors.

The same procedure was repeated for a gas phase HOD molecule in SPC/E water model geometry (OH and OD bond lengths of 1 Å and a HOD bond angle of 109.47°). Vibrational transition frequencies of the OH and OD stretches were calculated to be 3779 and 2788 cm^{-1}, respectively. The difference in water geometry between the TIP4P and SPC/E water models has just a small effect on the OH and OD vibrational frequencies. The ratio between the measured and calculated OH and OD vibrational frequencies yields multiplicative scale factors of 0.981 and 0.977, respectively. All of the OH and OD stretch vibrational frequencies of SPC/E HOD in D_2O and H_2O clusters were corrected using these scale factors.

Two sets of 100 small water clusters were chosen at random from 5 independent snapshots taken from MD simulations of neat TIP4P water and SPC/E water at 300 K (more details regarding the MD simulations are discussed in Sec. II C). The simulations contained 108 water molecules, and there was 200 ps of dynamics between each snapshot. For the purposes of choosing representative configurations of water clusters within the liquid, it was not necessary to simulate specifically HOD in H_2O or D_2O, because the equilibrium structure of the liquid does not depend on the mass of the molecules. Properly describing the vibrational properties of a water molecule in liquid water with electronic structure methods applied to a finite cluster is complicated by the ability of the water molecule to participate in extended hydrogen bond networks[77–85] and by the nonlinear cooperative effects of a water molecule simultaneously engaging in multiple hydrogen bonds.[86–88] Capturing these effects requires the use of a moderately large basis set that contains diffuse func-

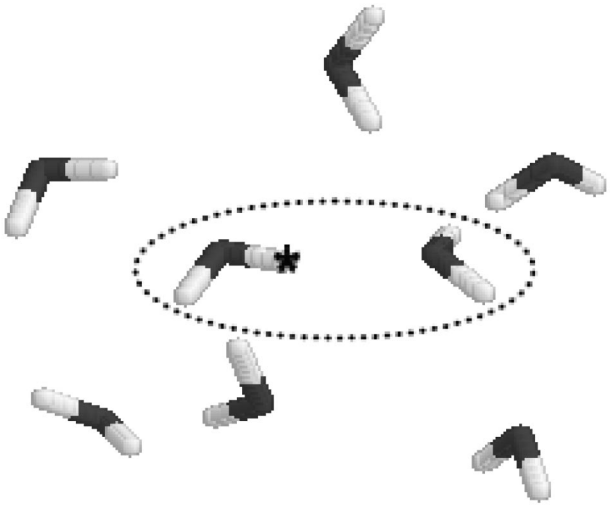

FIG. 2. Example of a typical TIP4P solvated dimer water cluster. The dotted line encircles the water dimer and the asterisk represents the OH (or OD) stretch of interest.

tions, e.g., the 6-311++G^{**} basis set, and sufficiently large clusters. We first attempted to analyze clusters containing a single solvation shell around the water molecule of interest. The size of these clusters was insufficient to recover enough of the approximately 300 cm^{-1} (225 cm^{-1}) solvent-induced redshift of the OH (OD) vibrational frequency of HOD. We found that it was important to choose clusters in which the hydrogen bond donor/acceptor pair (with the OH hydrogen or OD deuterium as the donor) was solvated.

We used the following procedure to choose the solvated dimer clusters from the neat water snapshots: (1) a water molecule was chosen at random; (2) one of the two OH stretches was chosen to be the vibration of interest; (3) the water molecule having an O atom closest to the H atom of the OH stretch of interest was chosen to be the second member of the dimer; (4) the water molecules having their O atoms closest to each of three remaining H atoms on the water dimer molecules were included in the cluster; (5) finally, any water molecule having one of its H atoms within 2.37 Å (approximately the first minimum in the OH radial distribution function for both SPC/E and TIP4P water) of either water dimer O atom was included in the cluster. A typical example of a TIP4P solvated dimer water cluster is shown in Fig. 2. The dotted oval encircles the water dimer, and the asterisk identifies the OH stretch of interest. The most common number of water molecules in a solvated dimer cluster is 8 (much like the example shown in Fig. 2), although they ranged in size from 5 to 10 water molecules.

For each of the 200 solvated dimer clusters, the one-dimensional *ab initio* potential energy curve for stretching the OH bond of interest from 0.72 to 1.28 Å was calculated. The electronic structure results do not depend on the isotopic mass of the atoms in the clusters. The curves were fit to the Morse function [Eq. (1)] and OH stretch frequencies [presuming $HOD\cdot(D_2O)_n$ clusters] and OD stretch frequencies [presuming $HOD\cdot(H_2O)_n$ clusters] were determined by applying Eqs. (2) and (3) with the appropriate choice of reduced mass. For the TIP4P clusters the average OH (OD) shift in stretch frequency from the gas phase was -255 cm^{-1} (-179 cm^{-1}) with standard deviation of 142 cm^{-1} (99 cm^{-1}). Similarly, for the SPC/E clusters the average OH (OD) shift in stretch frequency from the gas phase was -250 cm^{-1} (-176 cm^{-1}) with standard deviation of 144 cm^{-1} (101 cm^{-1}). For both water models the average OH (OD) frequency observed in the solvated dimer clusters recovers approximately 80% of the overall redshift measured experimentally for solvating a HOD molecule in liquid H_2O (D_2O). Larger clusters (perhaps those including a second solvation shell around the dimer) would recover even more of the redshift, but would be considerably more computationally expensive to analyze (at the same level of theory and basis set).

We also performed electronic structure calculations on the clusters inside a cavity in a dielectric medium (whose dielectric constant is that of water). For each cluster these calculations resulted in modest (less than 10%) changes in frequency. Certainly with this type of approach the average frequencies in the clusters would be expected to reproduce better the experimental frequencies in solution, and they do. But as described in Sec. II B where we correlate the frequency with the electric field from the solvent molecules, it is not necessarily more consistent to include this dielectric effect, and since it is relatively small anyway, we decided not to pursue it further.

B. Relationship between frequency and electric field

Next, we needed to develop an empirical relationship between the *ab initio* HOD stretch frequencies and the geometries of the solvation environments in the clusters. A simple way to characterize the solvation environment is by the electric field from the solvent molecules. In principle we could calculate this electric field from the *ab initio* charge density. However, since we wish to use the relationship between vibrational frequency and electric field within MD simulations, it is more convenient to develop the empirical relationship in terms of point charges on the solvent molecules for the SPC/E and TIP4P water models. We correlated the OH and OD stretch frequencies with the projection, E, of the electric field in atomic units (a.u.) along the OH (or OD) bond evaluated at the site of the H (or D) atom. Thus,

$$E=\hat{r}_{\mathrm{OH}}\cdot\sum_{i=1}^{3n}\frac{q_i\hat{r}_{iH}}{r_{iH}^2}, \tag{4}$$

where $\hat{r}_{\mathrm{OH}}$ is a unit vector that points from O to H in the direction of the OH (or OD) bond, the sum is over each of the three charged sites[89] of the n TIP4P or SPC/E water molecules that solvate the HOD molecule in the cluster, q_i is the charge of site i in a.u. ($e=1$), $r_{i\mathrm{H}}$ is the distance between site i and the H (or D) atom of the HOD molecule in a.u., and $\hat{r}_{i\mathrm{H}}$ is a unit vector that points from site i to the H (or D) atom of the HOD molecule.

Figure 3 shows a plot of the 100 *ab initio* TIP4P OH and OD stretch frequencies versus E. Also shown in Fig. 3 are fits of the OH and OD *ab initio* frequencies to a linear function of E,

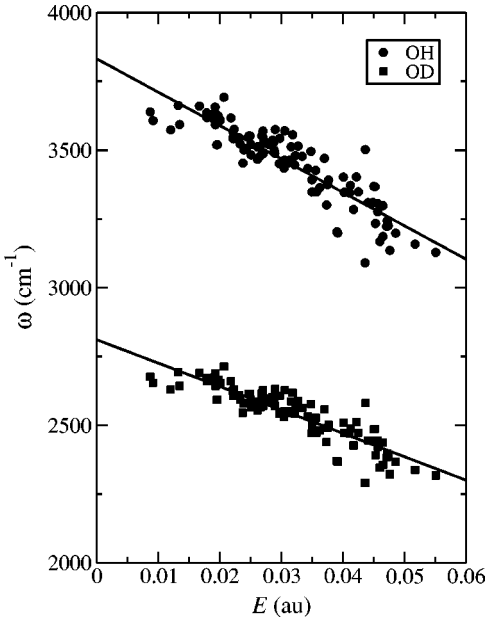

FIG. 3. Symbols indicate *ab initio* OH or OD vibrational frequencies of a HOD molecule in 100 D_2O or H_2O clusters chosen at random from a simulation of TIP4P water. These frequencies are plotted as a function of the electric field along the OH or OD bond due to the solvent water molecules in the cluster. The solid lines are linear fits to the data.

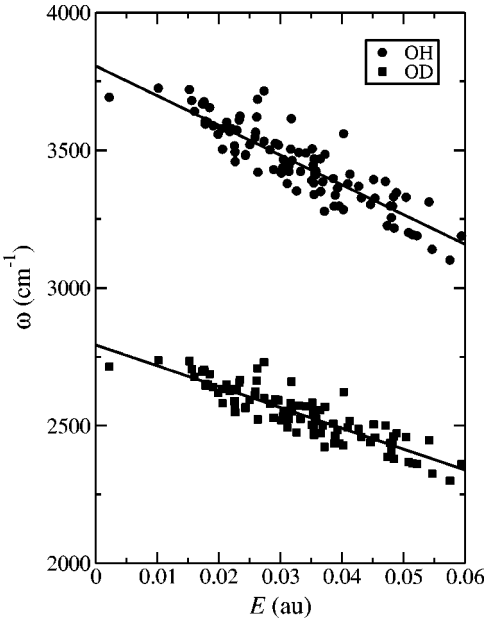

FIG. 4. Same as in Fig. 3, but for the SPC/E model of water.

$$\omega = a_0 + a_1 E, \tag{5}$$

where a_0 and a_1 are parameters of the fit, and ω is in units of cm^{-1}. For the OH stretch frequencies $a_0 = 3832\,cm^{-1}$ and $a_1 = -12141\,cm^{-1}$/a.u., and for the OD stretch frequencies $a_0 = 2811\,cm^{-1}$ and $a_1 = -8508\,cm^{-1}$/a.u. Both of the linear fits have correlation coefficients of 0.89. Equation (5) establishes the necessary relationship between the environment of a HOD molecule and its vibrational frequencies. In Sec. II C we will discuss the results of using Eq. (5) within a MD simulation of HOD in H_2O and D_2O to construct a frequency trajectory that can be analyzed to yield a number of spectroscopic observables.

Figure 4 shows a plot of the 100 *ab initio* SPC/E OH and OD stretch frequencies versus *E*. For the OH stretch frequencies $a_0 = 3806\,cm^{-1}$ and $a_1 = -10\,792\,cm^{-1}$/a.u., and for the OD stretch frequencies $a_0 = 2793\,cm^{-1}$ and $a_1 = -7560\,cm^{-1}$/a.u. Both of the linear fits again have correlation coefficients of 0.89. The intercept parameters (a_0) are similar for the two water models, whereas the slope parameters (a_1) differ more substantially. As we will see in Sec. III A the distribution of electric fields present in liquid water is slightly broader for the SPC/E water model than for the TIP4P water model. This difference in the distribution of fields results from the different locations and magnitudes of point charges employed in the two water models. Although the distributions of fields are different, the distributions of the *ab initio* OH and OD stretch frequencies generated from the clusters for the two water models are very similar. This situation results in different slope parameters for the two models.

By parameterizing the OH and OD stretch frequencies in terms of the electric field, we are not advocating that there is a *causal* relationship between the electric field applied and the shift in frequency. Indeed, if there were, one could calculate the shift as a Stark effect.[33] Hermansson[90] has calculated the response of the OH vibration of water at the MP4 level of *ab initio* theory with a large basis set as a function of the strength of a static homogeneous electric field applied parallel to one of the OH bonds. She finds, for example, that an electric field having magnitude of 0.032 a.u., which is the average field experienced by a water molecule in a TIP4P simulation, would produce a redshift of approximately 100 cm^{-1}. This suggests that the full redshift in the liquid (of more than 300 cm^{-1}) results from more than just the effects of the electric field, i.e., one must consider details of the changes in the electronic structure of the water molecule as it participates in multiple hydrogen bonds. It is also important to note that Eq. (5) applies only to obtaining HOD stretch frequencies in a cluster or condensed phase environment. For example, the zero-field intercepts do not correspond to the gas phase OH and OD vibrational frequencies of the HOD molecule, and the linear relationship between the frequency and electric field is not valid at small electric fields (which occur only very rarely in the middle of a cluster or in a condensed phase environment).

Buck, Buch, and co-workers have also obtained a relationship between the electric field and the vibrational frequency of water by fitting the experimental infrared spectra of $(H_2O)_7$ and $(H_2O)_8$ clusters.[58–60] Their sigmoidal form is somewhat different from the linear correlation shown in Figs. 3 and 4. However, the geometries of small water clusters sampled from the liquid can be quite different from optimized gas-phase water cluster geometries of the same size. The empirical relationships between frequency and field used in our work were developed to reproduce the OH and OD vibrational frequencies of a HOD molecule in liquid water. Cho and co-workers have advocated using an empirical relationship between the frequency and electrostatic

potential.[54–57] We found that a multiple linear regression fit of the OH and OD *ab initio* frequencies to the electrostatic potential at the three atomic sites within the HOD molecule had a correlation coefficient of 0.70 for the TIP4P model of water. Thus, despite having four parameters (instead of two), the electrostatic potential fit was considerably worse than the linear fit of the frequencies to the component of the electric field (correlation coefficient of 0.89), and so using the electrostatic potential-frequency relationship was not pursued further. We also tried a multiple linear regression fit of the frequencies to the three electric field components at each of the three atomic sites within the HOD molecule. This fit with some 10 parameters has a correlation coefficient of 0.91, and the components of the electric field on the H (or D) atom of interest (and in the direction of the O atom) were emphasized the most by the fit. Since this much more involved approach was only a marginal improvement over Eq. (5), we simply used the latter. However, for a larger solute molecule in which the frequencies of interest are not simple local modes of vibration but rather are delocalized normal modes, it would most likely be necessary to fit frequencies to electric field components at multiple sites within the molecule.

C. Molecular dynamics

MD simulations of HOD in both H_2O and D_2O were performed for the commonly used TIP4P (Ref. 68) and SPC/E (Ref. 69) water models. The simulations contained 1 HOD molecule and 107 H_2O or D_2O molecules. The size of the cubic simulation box was chosen to give the number density of water at 300 K ($3.32\times10^{28}\,m^{-3}$),[91] and periodic boundary conditions were employed. The electrostatic forces were calculated using an approximation to the Ewald sum,[92] and the equations of motion were integrated using the leap-frog algorithm[93] with a 1 fs time step for the HOD/D_2O simulations and a 0.5 fs time step for the HOD/H_2O simulations. The rotations were treated using quaternions.[94] Equilibration of the system temperature to 300 K was accomplished by periodically rescaling the velocities of the molecules until the desired temperature was maintained to within ±1 K for 80 ps without further adjustment of the velocities. All of the results described below were computed from 5 ns constant energy trajectories. OH or OD stretch frequencies of the HOD molecule were computed by calculating the total electric field vector at the site of the H or D atom including Ewald summation. The projection of the field along the OH or OD bond was taken, and the vibrational frequency was determined by Eq. (5).

III. RESULTS AND DISCUSSION

A. Hydrogen bond distance and electric field distributions

It has been previously established by several workers that there is a significant correlation between the OH vibrational frequency of a HOD molecule and the distance between the H atom and the closest O atom of a solvent water molecule (i.e., the hydrogen bond distance in most cases), $R_{H\text{-}O}$.[43–46,50,95] In Fig. 5 we demonstrate this correlation for these new results by plotting the joint probability distribution

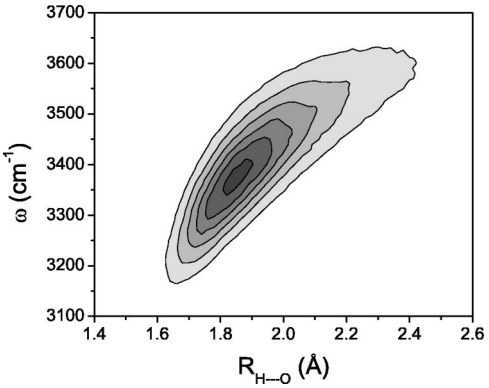

FIG. 5. Joint probability distribution of the OH stretch frequency, ω, of a HOD molecule in TIP4P D_2O vs the distance between the H atom and the nearest solvent O atom, $R_{H\text{-}O}$. The lines are equally spaced contours of constant probability.

for the OH stretch frequency of a HOD molecule in D_2O and $R_{H\text{-}O}$ for the TIP4P water model. Our results are very similar to those found earlier.[43–46] Qualitatively similar results hold for the SPC/E model and for the OD stretch frequency of HOD in H_2O. Short (strong) hydrogen bond lengths correspond to large redshifts in the vibrational frequencies. Conversely, long (weak) hydrogen bond lengths correspond to small redshifts in the vibrational frequencies. The relationship between frequency and hydrogen bond distance has important implications for molecular-level interpretation of the frequency fluctuation dynamics observed in various time-resolved ultrafast IR experiments. Since instantaneous frequency fluctuations correspond at least to some extent to fluctuations in the hydrogen bond length, it then follows that in spectral diffusion experiments one is observing, at least in part, the dynamics of the hydrogen bond distance fluctuations, including, for example, the formation and breaking of hydrogen bonds.[43–46]

It is also interesting to consider the overall distribution of electric fields present in an ensemble of HOD/H_2O or HOD/D_2O for both the TIP4P and SPC/E models. Since we are employing a linear expression that relates the electric field and the vibrational frequency, Eq. (5), the distribution of electric fields is trivially related to the distribution of frequencies, which represents the inhomogeneous limit of the IR absorption line shape (i.e., the IR absorption line shape without the effects of motional narrowing). While the distribution of frequencies is not an experimentally accessible quantity, it does provides information regarding the variety of solvent environments present in the liquid. In Fig. 6 we show the distribution of electric fields present in the TIP4P and SPC/E models (specific isotopic masses are not relevant to this calculation). Despite the different locations and magnitudes of the point charges in the two models, the distributions are similar in shape, and approximately Gaussian (although both distributions have a distinct shoulder at low fields, presumably from HOD molecules that are not hydrogen bonded through the H).[43] The average fields for the two distributions are 0.0365 a.u. for SPC/E and 0.0325 a.u. for TIP4P, and the standard deviation is $\sigma=0.0131$ and 0.0107 a.u., respectively. Overall, the SPC/E distribution is broader

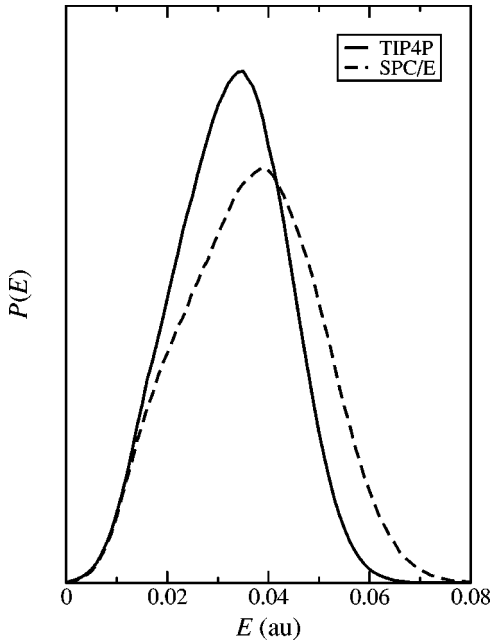

FIG. 6. Distributions of electric fields oriented along the OH bond for the TIP4P and SPC/E water models.

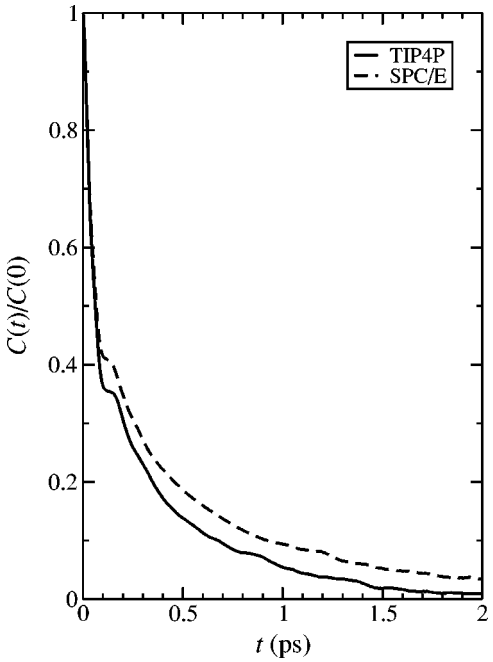

FIG. 7. OH stretch frequency fluctuation time-correlation functions for HOD in D_2O for both the TIP4P and SPC/E water models.

and contains, on average, slightly stronger fields. These differences in the distributions of electric fields between the two models result in differences (particularly in the slopes) in the empirical frequency-field relationships discussed in Sec. II B.

B. Frequency fluctuation dynamics

The time evolution of the vibrational frequencies of a HOD molecule in water provides a detailed measure of the dynamics of its solvation environment. In particular, the time scale for structural relaxation of the solvent (i.e., that makes and breaks hydrogen bonds) is probed by the OH (or OD) stretching vibration.[43–46] An important quantity that is accessible both to MD simulation and to time-dependent IR experiments is the equilibrium frequency fluctuation TCF,

$$C(t)=\langle \delta\omega(t)\,\delta\omega(0)\rangle, \tag{6}$$

where $\delta\omega(t)$ is the fluctuation of the instantaneous frequency from its equilibrium value, $\delta\omega(t)=\omega(t)-\langle\omega\rangle$. The time scales for the decay of $C(t)$ describe how quickly the frequency loses memory of its initial value (i.e., the time scales over which the molecule loses memory of its initial solvation environment). Assuming a linear relationship between the frequency and electric field, Eq. (5), it is easy to show that the frequency fluctuation TCF is proportional to the electric field fluctuation TCF,

$$C(t)=a_1^2\langle \delta E(t)\,\delta E(0)\rangle, \tag{7}$$

where $\delta E(t)$ is the fluctuation of the instantaneous electric field from its average value, $\delta E(t)=E(t)-\langle E\rangle$. Thus, within this formalism the normalized frequency TCF is identical to the normalized electric field TCF, and the latter is a property of the water model force field.

In Fig. 7 we show the normalized frequency TCF for the OH stretch vibration of HOD solvated in D_2O for both the TIP4P and SPC/E water models. For both solvent models there is initial fast decay (44 fs for TIP4P and 53 fs for SPC/E) and weak oscillation with a period of approximately 150 fs. The TCFs also exhibit long-time decay of about 0.5 ps for TIP4P and about 0.9 ps for SPC/E, which were determined by fitting the functions to an exponential for times greater than 1 ps. These normalized frequency TCFs agree well with previous theoretical calculations by several different groups using different methods to obtain the frequencies of the HOD molecule.[33,43–46,49] The fast decay and oscillation can be attributed to the underdamped hydrogen bond stretching motion between the HOD molecule and a D_2O molecule.[43–46,49,96–98] Recently, Fecko *et al.* made experimental measurements of the short-time decay and oscillation of the frequency TCF using vibrational echo peak shift spectroscopy with very short (52 fs) IR pulses.[33] They measured a fast decay of 60 fs and oscillation at 170 fs. Their results are in reasonable agreement with earlier theoretical predictions.[43–46]

Long-time decay of the frequency TCF has been attributed to the dynamics of forming and breaking hydrogen bonds.[43–46] A number of time-resolved ultrafast IR experiments have measured the asymptotic behavior of the frequency TCF, with results for the decay time ranging from 0.5 to 5 ps.[25,26,29–38] Our calculations show that long-time decays of the two water models differ by nearly a factor of 2, and are at the faster end of the range of experimentally measured time scales. It has been shown before that a number of dynamical quantities (e.g., rotations, self diffusion, etc.) of the SPC/E water model are slower than those of the TIP4P water model.[99] Since the frequency TCF probes structural relaxation of the solvent, it is not surprising that it would exhibit

slower dynamics for the SPC/E model than for the TIP4P model.

Fayer and co-workers[25,26] have used the frequency TCFs from this work as input to a perturbation theory calculation of two-dimensional vibrational echo correlation spectra of the OD stretch vibration of HOD in H_2O. (The normalized OD frequency TCF of HOD in H_2O is nearly identical to that of the OH stretch vibration of HOD in D_2O shown in Fig. 7.) Upon comparing the theoretical and measured spectra, these authors concluded that both the TIP4P and SPC/E models exhibit long-time dynamics that are too fast to reproduce accurately the results of the experiment, whose frequency TCF has a long-time decay of 2 ps. Since the frequency TCFs shown in Fig. 7 agree nearly quantitatively with those computed for the same water models using mixed quantum-classical methods,[43–46,49] it is reasonable to conclude that the frequency fluctuation dynamics presented here and elsewhere are accurate (for the model), and that any discrepancy with experiment is inherent to the water models themselves. A similar conclusion is found regarding rotational correlation times in water—the SPC/E model gives a correlation time about 30% too fast (compared to NMR experiments).[100] In fact, the SPC/E and TIP4P water models were not parameterized to reproduce the dynamics of water, but rather were designed to fit thermodynamic and structural properties of liquid water. There may now be sufficient experimental data and theoretical tools available to develop a new generation of water models that are parameterized to capture the structure, dynamics, and spectroscopy of liquid water. In particular, the polarizable TIP4P/FQ model recently developed by Rick *et al.*[101] shows great promise in that the hydrogen bond kinetics are considerably slower (and thus in better agreement with experiment) for this model than for the nonpolarizable TIP4P model.[102]

C. Vibrational line shapes

The OH and OD IR absorption line shapes of HOD in water contain information regarding both the structure and dynamics of the liquid. The absorption line shape is sensitive to the distribution of frequencies, which provides information about the different solvation environments present in the liquid. It is also sensitive to the time scales of the frequency fluctuation dynamics. A commonly used semiclassical approximation to the normalized absorption line shape is given by[49,61,103–106]

$$I(\omega)=\frac{1}{2\pi}\int_{-\infty}^{\infty}dt e^{-i\omega t}\phi(t), \tag{8}$$

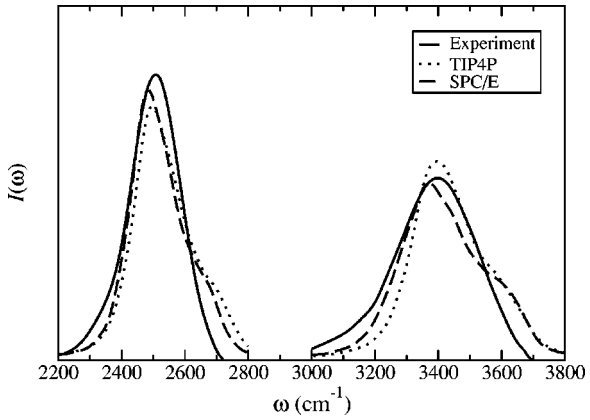

FIG. 8. OH (for HOD/D_2O) and OD (for HOD/H_2O) infrared absorption line shapes.

where

$$\phi(t)=e^{-|t|/T_1}\langle\hat{u}(0)\cdot\hat{u}(t)e^{i\int_0^t d\tau\delta\omega(\tau)}\rangle. \tag{9}$$

In the above expression $\hat{u}(t)$ is the instantaneous transition dipole moment unit vector in the molecular frame of reference, and T_1 is the population relaxation lifetime of the excited vibration. For the OH stretch of HOD in D_2O $T_1=750$ fs,[35,107,108] and for the OD stretch of HOD in H_2O $T_1=1.8$ ps.[47]

In Fig. 8 we compare with experiment[109] the normalized OD and OH absorption line shapes of HOD in H_2O and D_2O, respectively, calculated using Eq. (8) for both the TIP4P and SPC/E water models. One sees the calculated results for both water models are in quite good agreement with experiment. The calculated line shapes for both water models do, however, exhibit shoulders on the blue sides of the spectra that are not seen experimentally. This same shoulder was observed in previous theoretical investigations[49] (and in the electric field distributions in Fig. 6), and there is evidence that it represents the contribution to the line shape from a subensemble of OH or OD bonds whose hydrogen atom is not participating in a hydrogen bond.[44] We also note that the lifetime and rotational contributions to the line shape are minimal, but they were included for completeness.

The average frequencies, $\langle\omega\rangle$, full width at half maximum (FWHM), Γ, and solvent shift, $\Delta\omega=\langle\omega\rangle-\omega_g$, of the spectra shown in Fig. 8 are summarized in Table I. ω_g is the gas phase OH and OD frequency of the HOD molecule (3707 and 2724 cm^{-1}, respectively). Both the SPC/E and TIP4P models underestimate the experimental solvent shifts

TABLE I. Summary of the features of the experimental (Ref. 109) and theoretical infrared absorption line shapes. $\langle\omega\rangle$ is the average frequency, $\Delta\omega=\langle\omega\rangle-\omega_g$ is the difference between the average solution phase frequency and the gas phase frequency ($\omega_g=3707$ cm^{-1} for OH and 2724 cm^{-1} for OD), and Γ is the FWHM. All results are in cm^{-1}.

	Experiment			TIP4P			SPC/E		
	$\langle\omega\rangle$	$\Delta\omega$	Γ	$\langle\omega\rangle$	$\Delta\omega$	Γ	$\langle\omega\rangle$	$\Delta\omega$	Γ
OH Stretch	3400	−307	255	3445	−262	244	3418	−289	293
OD Stretch	2500	−224	170	2539	−185	179	2521	−203	171

TABLE II. Comparison of solvent shifts $\Delta\omega$ and linewidths Γ from different theoretical calculations for the OH stretch of HOD in D_2O. All results are in cm^{-1}.

Reference	$\Delta\omega$	Γ
51	−167	⋯
52	⋯	65
49	−312	163
46	−212	130
33	−257	⋯
Present work (TIP4P)	−262	244
Present work (SPC/E)	−289	293
Experiment	−307	255

for the OH and OD stretches: the SPC/E model by 6% for OH and 9% for OD, and the TIP4P model by 15% for OH and 17% for OD. Both models give linewidths that are in fair agreement with experiment. The largest discrepency between the calculated linewidths and experiment is seen for the SPC/E OH stretch calculation, which overestimates the width by 15%.

The comparison of these results to previous theoretical results for the line shift and width, for example, for the OH stretch of HOD in D_2O, is shown in Table II. One sees that the current results for both water models are generally in better agreement with experiment than the other results. The theoretical result for the linewidth was not reported by Fecko *et al.*,[33] but their FWHM for the frequency distribution is 270 cm^{-1}, and given the substantial amount of motional narrowing one can estimate that their linewidth would be about 150 cm^{-1}. All of these other theoretical results come from models where the frequency fluctuations arise from perturbations of the intramolecular OH stretch potential due to the usual point–charge and Lennard-Jones intermolecular interactions. One sees that the primarily electrostatic contributions in the results of the previous theories nearly uniformly underestimate the strength of the solvent-induced perturbations (since both the shifts and widths are too small), whereas the present electronic structure approach does a better job.

IV. CONCLUDING REMARKS

We have presented a new combined *ab initio*/MD approach to aid in the interpretation of ultrafast infrared spectroscopy of condensed phase systems. We have applied this approach to dilute mixtures of HOD in both H_2O and D_2O for two of the most commonly used models of water, TIP4P and SPC/E. The normalized frequency fluctuation TCFs we calculate for each water model are in good agreement with previous theoretical results, but differ somewhat from each other at long times. Moreover, they both appear to decay somewhat too fast (compared to experiment). The infrared absorption spectra are in reasonable agreement with experiment, and improve upon previous theoretical approaches, although the results for the two water models are slightly different. One general conclusion is that for hydrogen bonding systems electrostatic approaches, while qualitatively correct, miss some subtle but important electronic structure effects.

Assuming that the method we have developed to determine the vibrational frequency from a given solvent configuration is reliable, it follows that discrepancies between theory and experiment are then due to the water models themselves. In fact, the commonly used water models were not parameterized to reproduce the dynamics of water, but rather were designed to fit thermodynamic and structural properties. These new spectroscopic experiments, coupled with a reliable method for determining vibrational frequencies, provide additional dynamical benchmarks, and will perhaps lead to a new generation of water models that are parameterized to capture the structure, dynamics, and spectroscopy of liquid water.

Perhaps the most exciting aspect of our approach is that it can be easily applied to a host of other important problems relevant to chemistry, materials science, and biology. In a separate publication[110] we will describe the results of frequency fluctuation TCFs and infrared absorption line shapes for the amide I band of deuterated *N*-methylacetamide (NMA-D) in liquid D_2O computed using the methods described in this article. NMA-D has been extensively studied both experimentally and theoretically because it represents one of the simplest compounds that contains a peptide bond. We demonstrated that the empirical relationship between the electric field and frequency holds even for this larger molecule by performing a multiple linear regression fit of the amide I frequency to the three components of the electric field on each atom in the peptide bond. Frequency fluctuation TCFs and infrared line shapes were then computed with a MD simulation using the CHARMM[111] force field. These methods can also be applied to larger systems of biological relevance, which will provide molecular-level interpretation of present and future ultrafast infrared experiments. This is the subject of future research.

ACKNOWLEDGMENTS

The authors thank J. R. Schmidt and Frank Weinhold for helpful discussions. The authors are grateful for support by the National Science Foundation through Grant No. CHE-0132538. One of the authors (S.A.C.) also acknowledges support of a Ruth L. Kirschstein National Research Service Award administered through the National Institutes of Health.

[1] J. B. Asbury, T. Steinel, C. Stromberg, K. J. Gaffney, I. R. Piletic, A. Goun, and M. D. Fayer, Chem. Phys. Lett. **374**, 362 (2003).
[2] J. Bredenbeck and P. Hamm, J. Chem. Phys. **119**, 1569 (2003).
[3] M. Khalil, N. Demirdöven, and A. Tokmakoff, J. Phys. Chem. A **107**, 5258 (2003).
[4] A. T. Krummel, P. Mukherjee, and M. T. Zanni, J. Phys. Chem. B **107**, 9165 (2003).
[5] S. Woutersen, R. Pfister, P. Hamm, Y. Mu, D. S. Kosov, and G. Stock, J. Chem. Phys. **117**, 6833 (2002).
[6] O. Golonzka, M. Khalil, N. Demirdöven, and A. Tokmakoff, Phys. Rev. Lett. **86**, 2154 (2001).
[7] D. E. Thompson, K. A. Merchant, and M. D. Fayer, J. Chem. Phys. **115**, 317 (2001).
[8] S. Woutersen and P. Hamm, J. Chem. Phys. **115**, 7737 (2001).
[9] S. Woutersen and P. Hamm, J. Chem. Phys. **114**, 2727 (2001).
[10] M. T. Zanni, M. C. Asplund, and R. M. Hochstrasser, J. Chem. Phys. **114**, 4579 (2001).

[11] M. T. Zanni, S. Gnanakaran, J. Stenger, and R. M. Hochstrasser, J. Phys. Chem. B **105**, 6520 (2001).
[12] M. C. Asplund, M. T. Zanni, and R. M. Hochstrasser, Proc. Natl. Acad. Sci. U.S.A. **97**, 8219 (2000).
[13] A. Piryatinski, S. Tretiak, V. Chernyak, and S. Mukamel, J. Raman Spectrosc. **31**, 125 (2000).
[14] S. Woutersen and P. Hamm, J. Phys. Chem. B **104**, 11316 (2000).
[15] W. Zhao and J. C. Wright, Phys. Rev. Lett. **84**, 1411 (2000).
[16] P. Hamm, M. Lim, W. F. DeGrado, and R. M. Hochstrasser, Proc. Natl. Acad. Sci. U.S.A. **96**, 2036 (1999).
[17] P. Hamm, M. Lim, and R. M. Hochstrasser, J. Phys. Chem. B **102**, 6123 (1998).
[18] T. Wang, D. Du, and F. Gai, Chem. Phys. Lett. **370**, 842 (2003).
[19] C.-Y. Huang, Z. Getahun, Y. Zhu, J. W. Klemke, W. F. DeGrado, and F. Gai, Proc. Natl. Acad. Sci. U.S.A. **99**, 2788 (2002).
[20] C.-Y. Huang, J. W. Klemke, Z. Getahun, W. F. DeGrado, and F. Gai, J. Am. Chem. Soc. **123**, 9235 (2001).
[21] C.-Y. Huang, Z. Getahun, T. Wang, W. F. DeGrado, and F. Gai, J. Am. Chem. Soc. **123**, 12111 (2001).
[22] I. K. Lednev, A. S. Karnoup, M. C. Sparrow, and S. A. Asher, J. Am. Chem. Soc. **121**, 8074 (1999).
[23] P. A. Thompson, W. A. Eaton, and J. Hofrichter, Biochemistry **36**, 9200 (1997).
[24] S. Williams, T. P. Causgrove, R. Gilmanshin, K. S. Fang, R. H. Callender, W. H. Woodruff, and R. B. Dyer, Biochemistry **35**, 691 (1996).
[25] J. B. Asbury, T. Steinel, C. Stromberg, S. A. Corcelli, C. P. Lawrence, J. L. Skinner, and M. D. Fayer, J. Phys. Chem. A **108**, 1107 (2004).
[26] T. Steinel, J. B. Asbury, S. A. Corcelli, C. P. Lawrence, J. L. Skinner, and M. D. Fayer, Chem. Phys. Lett. (in press).
[27] Z. Wang, A. Pakoulev, Y. Pang, and D. Dlott, Chem. Phys. Lett. **378**, 281 (2003).
[28] R. Laenen, K. Simeonidis, and A. Laubereau, J. Phys. Chem. B **106**, 408 (2002).
[29] G. Gallot, N. Lascoux, G. M. Gale, J.-Cl. Leicknam, S. Bratos, and S. Pommeret, Chem. Phys. Lett. **341**, 535 (2001).
[30] J. Stenger, D. Madsen, P. Hamm, E. T. J. Nibbering, and T. Elsaesser, Phys. Rev. Lett. **87**, 027401 (2001).
[31] J. Stenger, D. Madsen, P. Hamm, E. T. J. Nibbering, and T. Elsaesser, J. Phys. Chem. A **106**, 2341 (2002).
[32] S. Yeremenko, M. S. Pshenichnikov, and D. A. Wiersma, Chem. Phys. Lett. **369**, 107 (2003).
[33] C. J. Fecko, J. D. Eaves, J. J. Loparo, A. Tokmakoff, and P. L. Geissler, Science **301**, 1698 (2003).
[34] S. Bratos, G. M. Gale, G. Gallot, F. Hache, N. Lascoux, and J.-Cl. Leicknam, Phys. Rev. E **61**, 5211 (2000).
[35] G. M. Gale, G. Gallot, F. Hache, N. Lascoux, S. Bratos, and J.-Cl. Leicknam, Phys. Rev. Lett. **82**, 1068 (1999).
[36] S. Woutersen and H. J. Bakker, Phys. Rev. Lett. **83**, 2077 (1999).
[37] R. Laenen, C. Rauscher, and A. Laubereau, Phys. Rev. Lett. **80**, 2622 (1998).
[38] R. Laenen, C. Rauscher, and A. Laubereau, J. Phys. Chem. B **102**, 9304 (1998).
[39] S. Woutersen, U. Emmerichs, and H. J. Bakker, Science **278**, 658 (1997).
[40] H. Graener, G. Seifert, and A. Laubereau, Phys. Rev. Lett. **66**, 2092 (1991).
[41] J. C. Deàk, S. T. Rhea, L. K. Iwaki, and D. D. Dlott, J. Phys. Chem. A **104**, 4866 (2000).
[42] A. Pakoulev, Z. Wang, and D. D. Dlott, Chem. Phys. Lett. **371**, 594 (2003).
[43] C. P. Lawrence and J. L. Skinner, Chem. Phys. Lett. **369**, 472 (2003).
[44] C. P. Lawrence and J. L. Skinner, J. Chem. Phys. **118**, 264 (2003).
[45] R. Rey, K. B. Møller, and J. T. Hynes, J. Phys. Chem. A **106**, 11993 (2002).
[46] K. B. Møller, R. Rey, and J. T. Hynes, J. Phys. Chem. A **106**, 1834 (2004).
[47] A. J. Lock and H. J. Bakker, J. Chem. Phys. **117**, 1708 (2002).
[48] C. P. Lawrence and J. L. Skinner, J. Chem. Phys. **117**, 5827 (2002).
[49] C. P. Lawrence and J. L. Skinner, J. Chem. Phys. **117**, 8847 (2002).
[50] J. R. Reimers and R. O. Watts, Chem. Phys. **91**, 201 (1984).
[51] L. Ojamäe, K. Hermansson, and M. Probst, Chem. Phys. Lett. **191**, 500 (1992).
[52] L. Ojamäe, J. Tegenfeldt, J. Lindgren, and K. Hermansson, Chem. Phys. Lett. **195**, 97 (1992).
[53] M. Diraison, Y. Guissani, J.-Cl. Leicknam, and S. Bratos, Chem. Phys. Lett. **258**, 348 (1996).
[54] M. Cho, J. Chem. Phys. **118**, 3480 (2003).
[55] S. Ham, J.-H. Kim, H. Lee, and M. Cho, J. Chem. Phys. **118**, 3491 (2003).
[56] K. Kwac and M. Cho, J. Chem. Phys. **119**, 2247 (2003).
[57] K. Kwac and M. Cho, J. Chem. Phys. **119**, 2256 (2003).
[58] J. Brudermann, M. Melzer, U. Buck, J. K. Kazimirski, J. Sadlej, and V. Buch, J. Chem. Phys. **110**, 10649 (1999).
[59] J. Sadlej, V. Buch, J. K. Kazimirski, and U. Buck, J. Phys. Chem. A **103**, 4933 (1999).
[60] U. Buck, I. Ettischer, M. Melzer, V. Buch, and J. Sadlej, Phys. Rev. Lett. **80**, 2578 (1998).
[61] D. W. Oxtoby, D. Levesque, and J.-J. Weis, J. Chem. Phys. **68**, 5528 (1978).
[62] A. Piryatinski, C. P. Lawrence, and J. L. Skinner, J. Chem. Phys. **118**, 9664 (2003).
[63] A. Piryatinski, C. P. Lawrence, and J. L. Skinner, J. Chem. Phys. **118**, 9672 (2003).
[64] C. P. Lawrence and J. L. Skinner, J. Chem. Phys. **119**, 1623 (2003).
[65] C. P. Lawrence and J. L. Skinner, J. Chem. Phys. **119**, 3840 (2003).
[66] T. Hayashi and H.-O. Hamaguchi, Chem. Phys. Lett. **326**, 115 (2000).
[67] R. B. Williams and R. F. Loring, Chem. Phys. **266**, 167 (2001).
[68] W. L. Jorgensen, J. Chandrasekhar, J. D. Madura, R. W. Impey, and M. L. Klein, J. Chem. Phys. **79**, 926 (1983).
[69] H. J. C. Berendsen, J. R. Grigera, and T. P. Straatsma, J. Phys. Chem. **91**, 6269 (1987).
[70] M. J. Frisch *et al.*, GAUSSIAN '98, Gaussian Inc., Pittsburgh, PA, 1998.
[71] A. D. Becke, J. Chem. Phys. **98**, 5648 (1993).
[72] C. Lee, W. Yang, and R. G. Parr, Phys. Rev. B **37**, 785 (1988).
[73] B. Miehlich, A. Savin, H. Stoll, and H. Preuss, Chem. Phys. Lett. **157**, 200 (1989).
[74] S. A. Corcelli, J. A. Kelley, J. C. Tully, and M. A. Johnson, J. Phys. Chem. A **106**, 4872 (2002).
[75] W. S. Benedict, N. Gailar, and E. K. Plyler, J. Chem. Phys. **24**, 1139 (1956).
[76] A. P. Scott and L. Radom, J. Phys. Chem. **100**, 16502 (1996).
[77] K. Modig, B. G. Pfommer, and B. Halle, Phys. Rev. Lett. **90**, 075502 (2003).
[78] G. Sutmann and R. Vallauri, J. Mol. Liq. **98**, 213 (2002).
[79] D. L. Bergman, Chem. Phys. **253**, 267 (2000).
[80] I. Ohmine and S. Saito, Acc. Chem. Res. **32**, 741 (1999).
[81] O. Mishima and H. E. Stanley, Nature (London) **396**, 329 (1998).
[82] A. Luzar and D. Chandler, Phys. Rev. Lett. **76**, 928 (1996).
[83] M. Matsumoto and I. Ohmine, J. Chem. Phys. **104**, 2705 (1996).
[84] E. Shiratani and M. Sasai, J. Chem. Phys. **104**, 7671 (1996).
[85] F. H. Stillinger, Science **209**, 451 (1980).
[86] F. Weinhold, J. Mol. Struct.: THEOCHEM **398–399**, 181 (1997).
[87] F. N. Keutsch and R. J. Saykally, Proc. Natl. Acad. Sci. U.S.A. **98**, 10533 (2001).
[88] J. D. Cruzan, L. B. Braly, K. Liu, M. G. Brown, J. G. Loeser, and R. J. Saykally, Science **271**, 59 (1996).
[89] In the TIP4P model of water there are three charged sites: one on each of the H atoms having charge of $0.52e$, and a third site with charge $-1.04e$ located 0.15 Å from the O atom on the C_2 axis (toward the H atoms). In the SPC/E model of water there are three atomic centered charged sites: the H atoms have charge of $0.4238e$, and the O atom has charge of $-0.8476e$.
[90] K. Hermansson, J. Chem. Phys. **99**, 861 (1993).
[91] *Water: A Comprehensive Treatise*, edited by F. Franks (Plenum, New York, 1972), Vol. 1.
[92] D. J. Adams and G. S. Dubey, J. Comput. Phys. **72**, 156 (1987).
[93] M. P. Allen and D. J. Tildesley, *Computer Simulation of Liquids* (Clarendon, Oxford, 1987).
[94] M. Svanberg, Mol. Phys. **92**, 1085 (1997).
[95] A. Novak, Struct. Bonding (Berlin) **18**, 177 (1974).
[96] D. M. Carey and G. M. Korenowski, J. Chem. Phys. **108**, 2669 (1998).
[97] J. T. Kindt and C. A. Schmuttenmaer, J. Chem. Phys. **106**, 4389 (1997).
[98] E. W. Castner, Jr., Y. J. Chang, Y. C. Chu, and G. E. Walrafen, J. Chem. Phys. **102**, 653 (1995).
[99] D. van der Spoel, P. J. van Maaren, and H. J. C. Berendsen, J. Chem. Phys. **108**, 10220 (1998).
[100] J. Ropp, C. Lawrence, T. C. Farrar, and J. L. Skinner, J. Am. Chem. Soc. **123**, 8047 (2001).
[101] S. W. Rick, S. J. Stuart, and B. J. Berne, J. Chem. Phys. **101**, 6141 (1994).

[102] H. Xu, H. A. Stern, and B. J. Berne, J. Phys. Chem. B **106**, 2054 (2002).
[103] M. D. Stephens, J. G. Saven, and J. L. Skinner, J. Chem. Phys. **106**, 2129 (1997).
[104] S. Mukamel, *Principles of Nonlinear Optical Spectroscopy* (Oxford, New York, 1995).
[105] J. G. Saven and J. L. Skinner, J. Chem. Phys. **99**, 4391 (1993).
[106] L. E. Fried and S. Mukamel, Adv. Chem. Phys. **84**, 435 (1993).
[107] S. Woutersen, U. Emmerichs, H.-K. Nienhuys, and H. J. Bakker, Phys. Rev. Lett. **81**, 1106 (1998).
[108] G. M. Gale, G. Gallot, and N. Lascoux, Chem. Phys. Lett. **311**, 123 (1999).
[109] M. Falk and T. A. Ford, Can. J. Chem. **44**, 1699 (1966).
[110] J. R. Schmidt, S. A. Corcelli, and J. L. Skinner (unpublished).
[111] A. D. MacKerell, Jr. *et al.*, J. Phys. Chem. B **102**, 3586 (1998).